J. metamorphic Geol., 2003, **21,** 515–522

Two stage growth of microdiamond in UHP dolomite marble from Kokchetav Massif, Kazakhstan

H. ISHIDA,[1] Y. OGASAWARA,[1] K. OHSUMI[2] AND A. SAITO[2]
[1]*Department of Earth Sciences, Waseda University, 1-6-1 Nishiwaseda, Shinjuku-ku, Tokyo 169–8050, Japan (yoshi777@waseda.jp)*
[2]*Institute of Materials Structure Science, KEK, 1–1 Oho, Tsukuba, Ibaraki 305–0801, Japan*

ABSTRACT The abundance and morphology of microdiamond in dolomite marble from Kumdy-kol in the Kokchetav Massif, are unusual; a previous study estimated the maximum content of diamonds in dolomite marble to be about 2700 carat ton^{-1}. Microdiamond is included primarily in garnet, and occasionally in diopside and phlogopite pseudomorphs after garnet. They are classified into three types on the basis of their morphology: (1) S-type: star-shaped diamond consisting of translucent cores and transparent subhedral to euhedral very fine-grained outer parts; (2) R-type: translucent crystals with rugged surfaces; and (3) T-type: transparent, very fine-grained crystals. The S-type is the most abundant.

Micro-Laue diffraction using a 1.6-μm X-ray beam-size demonstrated that the cores of the star-shaped microdiamond represent single crystals. In contrast, the most fine-grained outer parts usually have different orientations compared to the core. Laser–Raman studies indicate that the FWHM (Full Width at Half Maximum) of the Raman band of the core of the S-type diamond is slightly larger than that for the outer parts. Differences in morphology, crystal orientations, and in the FWHM of the Raman band between the core and the fine-grained outer-parts of S-type microdiamond suggest that the star-shaped microdiamond was formed discontinuously in two distinct stages.

Key words: dolomite marble; Kokchetav Massif; microdiamond; micro-Laue diffraction; ultrahigh-pressure metamorphism.

INTRODUCTION

Microdiamond in UHP metamorphic rocks can form in one of four settings: presolar, impact, crustal and mantle origins (Haggerty, 1999). The microdiamonds in the Kokchetav Massif, northern Kazakhstan are of crustal origin, formed during UHPM due to continental collision (Sobolev & Shatsky, 1990). The carbon sources for such microdiamond are thought to be a mixture of crustal carbonates and biogenic materials (De Corte *et al*., 1998, 2000). Subsequent to the first description of microdiamond of UHPM origin by Sobolev & Shatsky (1990), additional occurrences have been reported from several other UHP terranes – Dabieshan and Sulu in China (Xu *et al*., 1992), the Western Gneiss Region in Norway (Dobrzhinetskaya *et al*., 1995), Saxonian Erzgebirge in Germany (Massonne, 1998; Stöckhert *et al*., 2001), and the Bantimala complex of Sulaesi, Indonesia (Parkinson & Katayama, 1999). Microdiamond occurs in several rock types in the Kumdy-kol area of the Kokchetav Massif, including garnet-biotite gneiss, garnet–pyroxene rock, garnet–pyroxene–quartz rock, and impure dolomite-bearing carbonate rocks (e.g. Shatsky *et al*., 1995; Ogasawara *et al*., 2000).

Three types of UHPM carbonate rocks have been described in the Kumdy-kol area, diamond-bearing dolomite marble, diamond-free dolomitic marble and calcite marble (Ogasawara *et al*., 2000, 2002). Recently, exsolution of coesite from supersilicic titanite was reported in calcite marble indicating a minimum pressure of 6 GPa (Ogasawara *et al*., 2002). The concentration of microdiamond in dolomite marble was estimated to be about 2700 carat ton^{-1} (Yoshioka *et al*., 2001). The difference in the mineral assemblages in the two types of dolomite-bearing carbonate rock was explained by the local heterogeneity of fluid compositions, chiefly X_{CO_2} (Ogasawara *et al*., 2000).

Close relationships between diamond formation and C-H-O fluids are known from several experimental studies performed within the diamond stability field (Akaishi & Yamaoka, 2000; Kumar *et al*., 2000) and from investigations of natural microdiamond from Kokchetav UHP terrane (De Corte *et al*., 1998, 2000; Dobrzhinetskaya *et al*., 2001). Diamond was also synthesised in the presence of carbonate melt (e.g. Pal'yanov *et al*., 1999, 2002; Shatsky *et al*., 2001). These recent results on the formation of diamond indicate fluids and/or carbonate melts may play an important role in the formation of diamond. The purpose of this paper is to describe the microdiamond in dolomite marble from the Kokchetav Massif and to discuss their mechanism of formation.

METHODS

Crystal orientations of microdiamond in dolomite marble were examined by the micro-Laue diffraction method using X-rays (beam line no. BL-4B1) coupled with synchrotron radiation at the Photon Factory (PF) in the High Energy Accelerator Research Organization, Tsukuba, Japan. The main part of the injector of electrons or positrons is a 400-m long linear accelerator. Diffraction using monochromatic X-ray radiation is too weak to obtain clear diffraction patterns at the scale of micrometres. As the Laue method uses continuous X-rays, coupling with synchrotron radiation generates strong diffraction patterns, even from a micrometre size area. Using the beam line BL-4B1 at PF, a continuous X-ray beam was focused to a minimum beam diameter of 1.6 μm, using three slits and a micro pin hole (MP) (Ohsumi, 1997). Acquisition time for each sample was 30–60 min for beams of 1.6 and 6 μm diameter, and 10 s for a beam of 50 μm diameter. This micro-Laue diffraction instrument uses standard polished thin sections, and digital Laue diffraction images of microdiamond and their host minerals can be obtained *in-situ*. The indices of Laue reflections were determined using a computer program.

Microdiamond in dolomite marbles were also examined by laser Raman spectroscopy with a JASCO NRS-2000 spectrophotometer at Tokyo Institute of Technology. The excitation was provided by a 514.54-nm line of an Ar-ion laser at 30 mW. The laser beam was focused to a spot size of 1 μm. For measurement of FWHM (Full Width at Half Maximum) of the Raman band of diamond, background intensities were determined at -100 to $+100$ cm^{-1}.

PETROLOGY OF DIAMOND-BEARING DOLOMITE MARBLE

The UHP rocks of the Kumdy-kol area, Kokchetav Massif consist mainly of gneiss and eclogite (e.g. Sobolev & Shatsky, 1990; Kaneko *et al.*, 2000; Katayama *et al.*, 2000; Okamoto *et al.*, 2000) with minor amounts of impure carbonate rock (e.g. Ogasawara *et al.*, 2000). These metamorphic rocks in the Kumdy-kol area belong to Unit II of the geological map by Kaneko *et al.* (2000). Two types of dolomite-bearing marbles occur in this area; one in which dolomite is dominant carbonate is diamond-bearing and the other in which Mg-calcite and dolomite occur is diamond-free (Ogasawara *et al.*, 2000). These two marbles were subjected to the same *P-T* conditions; their difference in mineral assemblages, including the presence or absence of diamond, can be explained by local heterogeneity of fluid compositions, particularly X_{CO_2}, during UHPM (Ogasawara *et al.*, 2000). Another interesting UHP carbonate rock is a calcite marble that contains titanite with coesite exsolution needles and plates. Excess Si contents prior to the coesite exsolution yield a minimum metamorphic pressure of 6 GPa (Ogasawara *et al.*, 2002).

Dolomite marble consists mainly of dolomite (60 vol%), diopside (15 vol%), garnet ($<$ 10 vol%), and phlogopite (10 vol%), with minor amounts of low-Mg calcite, microdiamond and graphite, and has a granoblastic texture (Fig. 1a). Textural relations indicate that the peak assemblage is Dol (+ Arg) + Di + Grt + Dm. This rock contains abundant microdiamond ± graphite, mainly in garnet, and sometimes in diopside and phlogopite

Dolomite occurs in the matrix and as inclusions in garnet and diopside. Dolomite in the matrix occurs as anhedral crystals, with grain sizes ranging from 0.5 to 1.0 mm in the longest dimension. Numerous polycrystalline aggregates of graphite (5–30 μm) are included in matrix dolomite.

Garnet (0.7–5 mm in longer dimension) forms anhedral, granular-shaped crystals, and is often rimmed by later stage phlogopite and calcite. Garnet

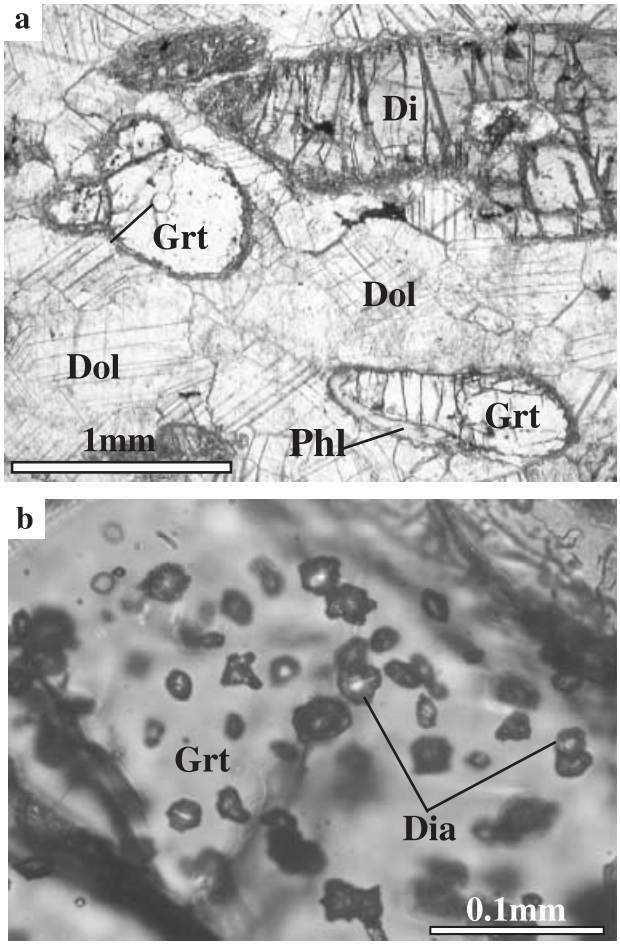

Fig. 1. (a) Photomicrograph of diamond-bearing dolomite marble. Plane-polarized light. Grt: garnet, Di: diopside, Dol: dolomite, Phl: phlogopite. (b) Photomicrograph of microdiamonds in garnet at high concentration part. Plane-polarized light. Dia: diamond.

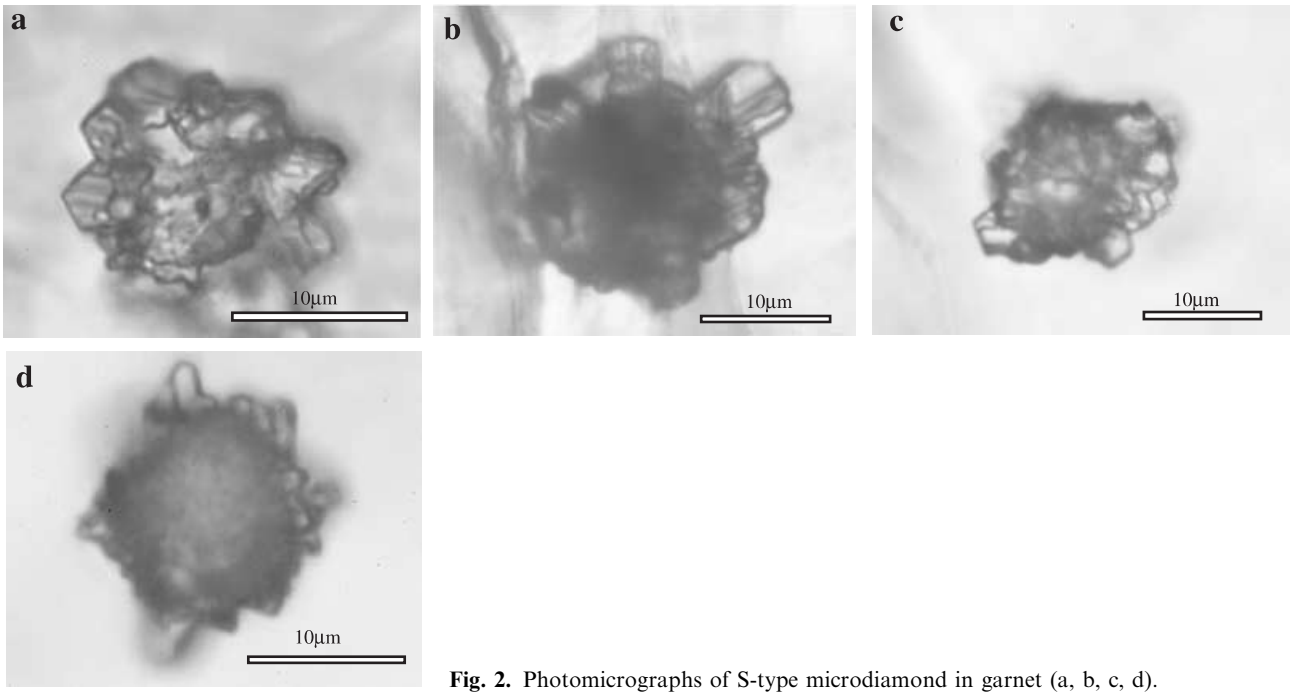

Fig. 2. Photomicrographs of S-type microdiamond in garnet (a, b, c, d).

contains abundant microdiamond frequently coexisting with anhedral fine-grained graphite (5–30 μm). Low-Mg calcite, almost pure calcite and dolomite are included in garnet and diopside. They have globular, rounded forms, and are usually 0.1 mm in size.

Diopside (0.4–2.5 mm in long dimension) forms anhedral to subhedral prismatic crystals. Some diopside grains are rimmed by tremolite + Mg-calcite of secondary origin. Tremolite also occurs along cleavage traces of diopside. Diopside grains contain exsolution needles of phengite (determined by laser Raman spectroscopy) and inclusions of microdiamond and graphite.

Phlogopite is a secondary mineral that occurs as aggregates in the matrix and as reaction rims surrounding garnet. Whereas the matrix phlogopite aggregates (0.5–1.0 mm in diameter) do not contain any diamond or graphite, phlogopite reaction rims (0.2–0.3 mm wide) typically contain microdiamond and graphite inherited from the former garnet. Euhedral graphite, relatively coarse-grained (0.1 mm in long dimension) is observed in calcite layers, and is a late-stage precipitate from fluids during exhumation.

MICRODIAMOND IN DOLOMITE MARBLE

Some 4458 grains of microdiamond inclusions were counted on four polished thin sections (about 30 μm in thickness) of dolomite marble. The diamond is found mainly in garnet, less frequently in diopside and phlogopite-bearing pseudomorphs after garnet, and rarely in phengite and carbonate minerals. The average grain size of the microdiamond is 10–15 μm, and they range from 5 to 25 μm in size. The maximum size is about 60 μm in long dimension. Some garnet grains contain unusually high concentrations of microdiamonds. The area of the highest concentration is shown in Fig. 1(b). The grain size of microdiamonds in the area with the highest concentration is slightly smaller ($\bar{x} = 10$ μm in diameter) than that in other parts of garnet. The distribution of microdiamond in garnet is heterogeneous. Polycrystalline aggregates (5–30 μm) of graphite are included in garnet, diopside, phlogopite and dolomite. Many microdiamond are partially surrounded by late-stage graphite.

The diamonds are classified into three types according to their petrographic morphology as based on analysis of 1688 grains from all of the counted grains, namely: (i) S-type (star-shaped), (ii) R-type (rugged face) and (iii) T-type (transparent and very fine-grained).

S-type microdiamond (about 85%)

Most of the microdiamond (1442 grains) in dolomite marble are of S-type. Representative photomicrographs of S-type microdiamond are shown in Fig. 2. They are characterized by a translucent core of about 5–20 μm in diameter and a marginal area consisting of fine-grained (about 1–5 μm) subhedral to euhedral transparent microdiamond with well developed crystal faces; some are thin plates. Morphology, size, surface and translucent appearance of the core are similar to the R-type, whereas the marginal areas are in turn similar to those of T-type. Such a morphological feature of a coarse-grained core with an outer fine-grained rim suggests the cores represent seed crystals for a later overgrowth.

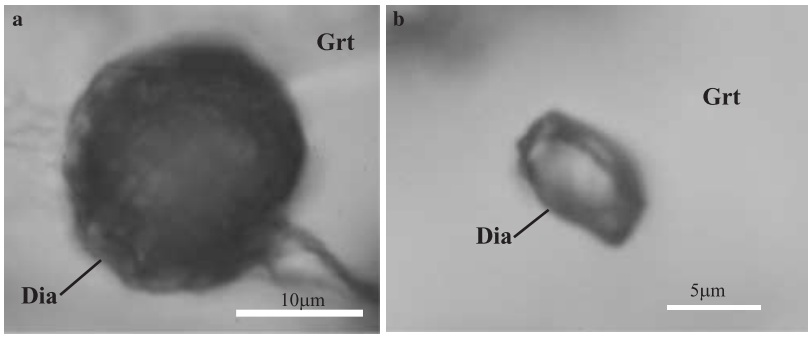

Fig. 3. Photomicrographs of R-type (a) and T-type (b) microdiamond. Grt: garnet, Dia: diamond.

Table 1. Experimental conditions and the results of micro-Laue diffraction of microdiamond.

Types	Sample no.	X-ray beam sizes, the number of analyzed spots and time intervals			Results* Number of orientations
		1.6 μm	6 μm	50 μm	
S	xx1dia2	4 spots t = 30 min	1 spot t = 60 min		3: C + R(2)
S	xx1dia5	7 spots t = 30 min	5 spots t = 30 min		2: C + R(1)
S	xx1dia10	9 spots t = 30 min	9 spots t = 30 min		3: C + R(2)
S	xx1dia13	16 spots t = 30 min			2: C + R(1)
R	c43dia2		3 spots t = 60 min	1 spot t = 10 s	1
R	xx1dddia1	2 spots t = 30 min			2: C + R(1)
R	zw47dia2		1 spot t = 60 min	1 spot t = 10 s	1

* Results.
C: the core part. R: different orientated outer part. (n): n is the number of orientations detected from outer part.

R-type (about 10%)

R-type microdiamond (Fig. 3a) has a rugged surface and is generally translucent. Crystals measure 5–20 μm in diameter. Their shapes are round to slightly angular. Some of them resemble cuboids. This type (179 grains) is characterized by a relatively large-grained core with very thin rims.

T-type (< 5%)

T-type microdiamond (Fig. 3b) is transparent and very fined-grained (1–7 μm in diameter). They are angular or slightly angular with smooth surfaces. This type (67 grains) of microdiamond is characterized by the lack of a discernible core domain.

MICRO-LAUE X-RAY DIFFRACTION OF MICRODIAMOND

Microdiamond of two different types (S & R), all of which have been studied previously by laser Raman spectroscopy, together with graphite, garnet and dolomite were examined by micro-Laue X-ray diffraction (Table 1). Clear Laue patterns were obtained in each sample for S-type microdiamond (51 Laue patterns of 4 grains). Laue reflections of the host minerals are generally superimposed upon those of the microdiamond as shown in Figs 4, 5 and 6.

Typical micro-Laue diffraction patterns for S-type microdiamond in garnet are shown in Fig. 4 with the reflections without indices being attributed to the host garnet. In the microdiamond grain shown in Fig. 4, three different orientations of microdiamond were detected. One represents the orientation of the core (Fig. 4b), and the other two (Fig. 4c) are attributed to its fine-grained rim. All Laue reflections of the core belong to one single orientation indicating the core is a single crystal. The Laue patterns of the fine-grained outer part show two different orientations (Fig. 4c), which indicate that even a very thin X-ray beam of 1.6 μm covered two grains. Laue patterns of the outer parts of S-type microdiamond are often mixed with those of the core, and their orientations are generally different (Figs 4c & 5). Laue patterns of some rim parts show the same orientation compared to the core (Fig. 4d). The spot d of Fig. 4 has only five Laue reflections of diamond attributed to one orientation the same as the core (Fig. 4b).

Laue reflections of a certain index of microdiamond included in garnet sometimes split into 2–5 weak reflections within a very narrow area, whereas Laue reflections of microdiamond in phlogopite are very clear and do not split. Sometimes, Laue reflections of the host garnet near a microdiamond grain split into two or three reflections.

R-type microdiamond (eight analyses of three grains) was examined using beam diameters of 1.6, 6, 50 μm respectively. Laue patterns have been obtained for R-type microdiamond. A clear pattern using an X-ray beam of 50 μm in diameter is shown in Fig. 6. This Laue pattern has only one orientation, and so the entire R-type diamond represents a single crystal. As the thickness of the outermost rugged area is very small (< 1 μm), it was difficult to obtain Laue patterns of the rim part of R-type. Only one pattern was obtained from the rim of R-type (Table 1).

LASER RAMAN SPECTROMETRY OF MICRODIAMOND

All three types of microdiamonds were also analyzed by laser Raman spectroscopy. For S- and R-types, the same analytical points used for the micro-Laue diffraction were chosen for the Raman study. In particular we paid attention to the FWHM of the strongest Raman band of diamond, at 1330–1335 cm^{-1}. No relation between the positions of the strongest peak and the types of microdiamond was detected. All Raman bands of diamond show strong intensity. A representative Raman spectrum of S-type microdiamond (outer part) is shown in Fig. 7. Some spectra for the rim part of S-type contained the Raman bands of graphite.

The values of FWHM of the Raman band of the core parts of S-type microdiamond range from 6.2 to 8.0 cm^{-1}; those of the outer parts are slightly smaller, ranging from 5.9 to 7.5 cm^{-1} (Table 2)

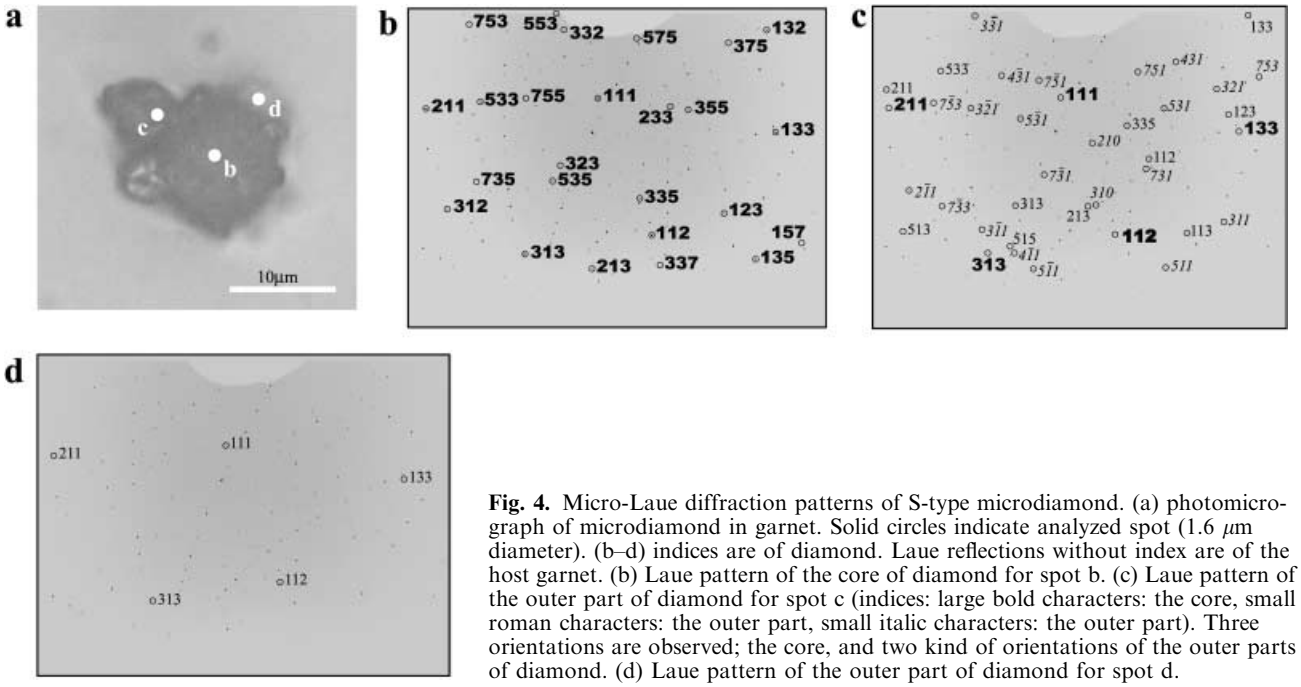

Fig. 4. Micro-Laue diffraction patterns of S-type microdiamond. (a) photomicrograph of microdiamond in garnet. Solid circles indicate analyzed spot (1.6 μm diameter). (b–d) indices are of diamond. Laue reflections without index are of the host garnet. (b) Laue pattern of the core of diamond for spot b. (c) Laue pattern of the outer part of diamond for spot c (indices: large bold characters: the core, small roman characters: the outer part, small italic characters: the outer part). Three orientations are observed; the core, and two kind of orientations of the outer parts of diamond. (d) Laue pattern of the outer part of diamond for spot d.

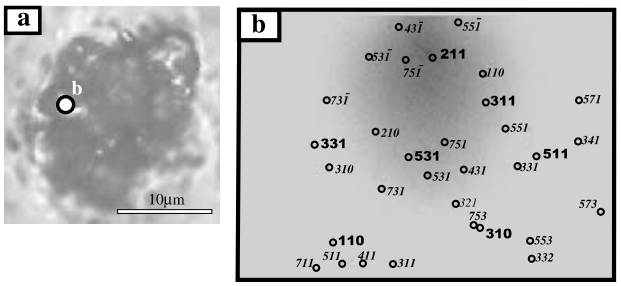

Fig. 5. Micro-Laue diffraction pattern of the outer part of S-type microdiamond. (a) photomicrograph: the position of the X-ray beam (1.6 μm diameter) is indicated by a solid circle. (b) Laue pattern for spot b. Laue reflections without index are of the host garnet. Two different orientations of the core (indices: large bold characters) and the outer part (indices: italic characters) are mixed.

except for the microdiamond associated with graphite. The difference in FWHM between the core and its surrounding part is usually 0.5–1.0 cm^{-1} in each grain. No correlation between the FWHM and the position of the strongest peak was detected.

R-type and T-type microdiamond have FWHM values ranging from 6.1 to 7.2 cm^{-1} and 5.1 to 5.7 cm^{-1} (nine analyses of three grains), respectively. The FWHM of T-type microdiamonds is smaller than both the core part of S-type microdiamond and the outer part (Table 2). In all of these Raman spectra, no interference by graphite or other extra phases were observed.

DISCUSSION TWO-STAGE GROWTH OF MICRODIAMOND

Understanding the growth mechanism of the most common S-type microdiamond and its relation to the other types is the key for understanding the process

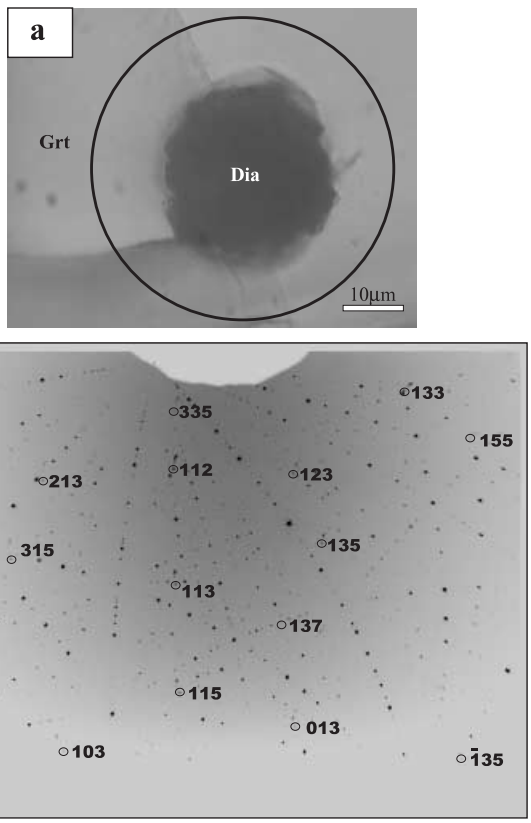

Fig. 6. Micro-Laue diffraction patterns of R-type microdiamond. (a) photomicrograph of R-type microdiamond. Circle indicates X-ray beam (50 μm). Grt: garnet, Dia: diamond. (b): Laue pattern of the area irradiated. Reflections without indices are of host garnet. All other reflections with indices are attributed to diamond and indicate one orientation.

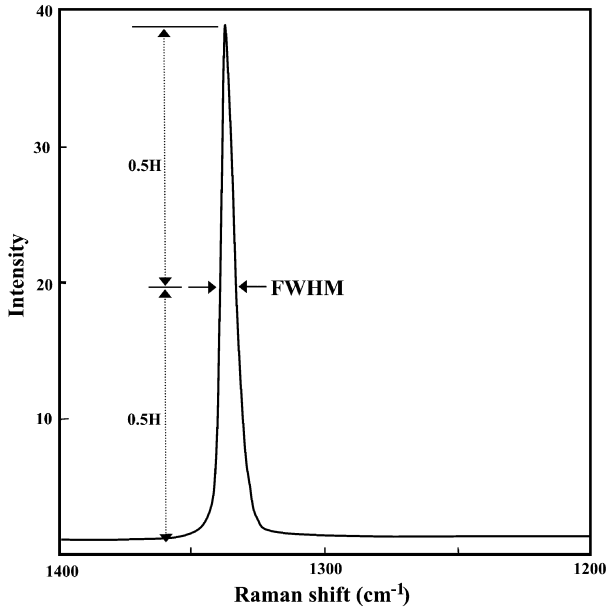

Fig. 7. Laser Raman spectrum of the outer part of S-type microdiamond.

of microdiamond formation in dolomite marble. The cores of S-type and R-type are translucent single crystals, and are relatively coarse-grained compared to T-type and the fine-grained outer parts of S-type. These features strongly suggest discontinuous growth of S-type microdiamond. Notably, two different crystal orientations and different FWHM's of the Raman band between the core and the outer part of S-type microdiamond are observed. Laue patterns proved that the core is a single crystal and that its outer part generally shows different orientations compared to the core. In each S-type grain, FWHM's of the Raman band of the cores are slightly larger than those of the fine-grained outer parts, independent of whether the outer parts have the same orientation as the core or not. These differences between the core and its outer part suggest that S-type microdiamond in dolomite marble did not grow continuously starting from a single seed crystal, but were formed discontinuously by a multistage process: the first stage (core formation) and the second stage (rim formation). During the second stage, the core part acted as a seed crystal for the growth of rims.

Katayama *et al.* (2000) described composite inclusions of relict prograde graphite and microdiamond in garnet in gneiss from Kumdy-kol. Diamond grew at the expense of graphite during the prograde stage. However, such composite grains were not found in the dolomite marble, which indicates that the growth mechanism of these microdiamond is different from that in the gneiss as reported by Katayama *et al.* (2000).

The two-stage growth model is not consistent with the formation of both core and rims of S-type microdiamonds exclusively by transformation from graphite. Rim diamond requires an additional source of carbon with a possible source being a fluid available during UHPM. The coexistence of microdiamond with phengite and carbonate suggests the crystallization of microdiamond occurred from a multicomponent fluid, as described by Stöckhert *et al.* (2001). Two kinds of composite inclusions were commonly found in garnet in dolomite marble; diamond-phengite (Fig. 8) and diamond–carbonate. These associations imply both the presence of a CO_2-H_2O mixed fluid with other components, and an intimate relationship between this fluid and diamond formation.

There have been several recent studies showing that C–O–H fluids play an important role during the formation of diamond both from experiments and in nature. Diamond, for instance, was synthesised within the diamond stability field in the presence of a CO_2–H_2O fluid at H_2O-rich compositions (Akaishi & Yamaoka, 2000; Kumar *et al.*, 2000). De Corte *et al.* (1998, 2000) described H_2O and carbonate inclusions in microdiamond using micro infrared spectroscopy. Dobrzhinetskaya *et al.* (2001) suggested the possibility of the diamond growth from C–O–H fluid in a garnet-biotite-feldspar gneiss from Kumdy-kol. Stöckhert *et al.* (2001) found multiple silicate inclusions in apparent equilibrium with microdiamonds in

Table 2. FWHM of Raman band of microdiamond.

Sample no.	Type	Core/outer part of S-type	The number of samples for each FWHM (cm^{-1}) range (#: including graphite)							
			5.1–5.5	5.6–6.0	6.1–6.5	6.6–7.0	7.1–7.5	7.6–8.0	8.1–8.5	8.6–9.0
xx1dia2	S	core part			1					
		outer part		2	1					
xx1dia5	S	core part				1	1			
		outer part		1	2					
xx1dia10	S	core part					2			
		outer part			2	2	1#		1#	1#
xx1dia13	S	core part						2		
		outer part					3	1#		1#
xx1dddia1	R						2			
zw47dia2	R				2	3				
xx1c1adia1	T		3							
xx1c1adia3	T			3						
zw47adia1	T		2	1						

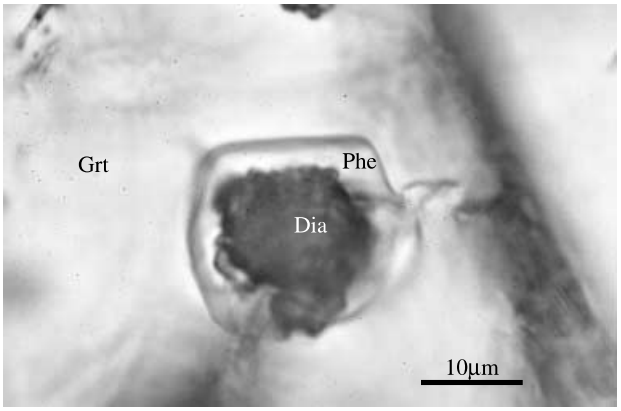

Fig. 8. Composite inclusion of diamond (S-type) + phengite in garnet in dolomite marble. Grt: garnet, Dia: diamond, Phe: phengite.

garnet in a UHP gneiss from Erzgebirge, Germany. They interpreted that these inclusions were originally a C–O–H fluid with other components and that diamond precipitated as a daughter crystal. All these studies have emphasized the close relationship between fluids and diamond formation.

Core crystals of S-type diamond have more potential sources; the coarse grain size and translucent character are important distinctions from its rims, as well as from T-type. If the core were transformed into diamond from graphite, one of the possible carbon sources for graphite was biogenic material. De Corte *et al*. (2000) argued that the Kokchetav microdiamond might have been a mixture of crustal carbonate and reduced carbonaceous material based on carbon isotopic data. If microdiamond cores were crystallized directly from a fluid during UHPM, then a different fluid to that of the second stage is required to explain the two-stage growth of microdiamond. We do not, at present, have any data to confirm the participation of two different fluids during the growth of diamond.

The similarity between the T-type microdiamond and the outer part of the S-type microdiamond (small FWHM of Raman band, small grain size, transparency, smooth surfaces), suggests that T-type microdiamond could have crystallized directly from a fluid without seed crystals.

Considering the similarity of the R-type and the core of the S-type (relatively large grain size and translucent character), R-type might be an early product formed at the beginning of the second stage prior to the growth of S-type diamond, possibly representing an embryo for the S-type. The rugged parts of R-type microdiamond might be very fine-grained overgrowths from fluid on the core.

CONCLUSIONS

High concentrations of metamorphic microdiamond occur as inclusions in garnet, diopside and phlogopite in dolomite marble from Kumdy-kol in the Kokchetav UHP massif of northern Kazakhstan. The microdiamonds are classified into three types on the basis of the morphology: S-type (star-shaped), R-type (rugged surface) and T-type (transparent). The S-type comprises about 85% of the microdiamond in dolomite marble, and consists of a core part and an outer fine-grained part, having subhedral to euhedral form.

Micro-Laue diffraction patterns of microdiamond shows that (1) the cores of S-type are single crystals (2) the outer parts have, for the most part, different orientations compared to the core (3) the main part of R-type is a single crystal. The FWHM of the Raman band of a core of S-type microdiamond is slightly larger than that of the fine-grained outer aggregate.

Differences in morphology, crystal orientation and FWHM of Raman band between the core and the outer parts indicate that S-type microdiamond were formed discontinuously during two different stages. The first stage formed the core and the second stage formed surrounding parts using the core as a seed crystal. Therefore, it is unlikely that the outer parts formed simply by transformation from graphite. More probably, these outer diamond were precipitated from a fluid during the second stage. Likewise, T-type microdiamond might also be formed directly from a fluid during this later stage.

ACKNOWLEDGEMENTS

The authors thank H.-P. Schertl, L. Dobrzhinetskaya, J. G. Liou, J. B. Noblett and C. Parkinson for their reviews and suggestions for improving this paper. We are grateful to S. Maruyama for laser Raman spectrometry, to M. Mukai for the experiment at BL-4B1 in PF of KEK, and to K. Saga and K. Yonemochi for their assistance in the laboratory studies. This study was financially supported in part by the Waseda University Grant for the Special Research Project no. 99 A-518, no. 2001 A-533, the Grant of RISE of Waseda University Project no. B-240 and the Grant in Aid of the Ministry of Education and Science no. 13640485.

REFERENCES

Akaishi, M. & Yamaoka, S., 2000. Crystallization of diamond from C-O-H fluids under high-pressure and high-temperature conditions. *Journal of Crystal Growth*, **209,** 999–1003.

De Corte, K., Cartigny, P., Shatsky, V. S., Sobolev, N. V. & Javoy, M., 1998. Evidence of fluid inclusions in metamorphic microdiamonds from the Kokchetav massif, northern Kazakhstan. *Geochimica et Cosmochimica Acta*, **62,** 3765–3773.

De Corte, K., Korsakov, A., Taylor, W. R., Cartigny, P., Ader, M. & De Paepe, P., 2000. Diamond growth during ultrahigh-pressure metamorphism of the Kokchetav Massif, northern Kazakhstan. *Island Arc*, **9,** 428–438.

Dobrzhinetskaya, L., Eide, E., Korneliussen, *et al*., 1995. Diamond in metamorphic rocks of the Western Gneiss region in Norway. *Geology*, **23,** 597–600.

Dobrzhinetskaya, L. F., Green, H. W. L., Mitchell, T. & Dickerson, R. M., 2001. Metamorphic diamonds: mechanism of growth and inclusion of oxides. *Geology*, **29,** 263–266.

Haggerty, S. E., 1999. A diamond trilogy: superplumes, supercontinents, and supernovae. *Science*, **285,** 851–860.

Kaneko, Y., Maruyama, S., Terabayashi, M., *et al*., 2000. Geology of the Kokchetav ultrahigh-pressure-high pressure metamorphic belt, north-eastern Kazakhstan. *Island Arc*, **9,** 264–283.

Katayama, I., Zayachkovsky, A. & Maruyama, S., 2000. Prograde pressure-temperature records from inclusions in zircons from ultrahigh-pressure-high-pressure rocks of the Kokchetav Massif, northern Kazakhstan. *Island Arc*, **9,** 417–427.

Kumar, M. D. S., Akaishi, M. & Yamaoka, S., 2000. Formation of diamond from supercritical H_2O-CO_2 fluid at high pressure and high temperature. *Journal of Crystal Growth*, **213,** 203–206.

Massonne, H. J., 1998. A new occurrence of microdiamonds in quarzofeldspathic rocks of Saxonian Erzgebirge, Germany, and their metamorphic evolution. *International Kimberlite Conference Extended Abstracts*, Cape Town, 552–554.

Ogasawara, Y., Fukasawa, K. & Maruyama, S., 2002. Coesite exsolution from supersilicic titanite in UHP calcite marble. *American Mineralogist*, **87,** 454–461.

Ogasawara, Y., Ohta, M., Fukasawa, K., Katayama, I. & Maruyama, S., 2000. Diamond-bearing and diamond-free metacarbonate rocks from Kumdy-kol in the Kokchetav Massif, northern Kazakhstan. *Island Arc*, **9,** 400–416.

Ohsumi, K., 1997. Structural studies on a sub-micrometer crystal grain and micrometer-sized area. *Journal of the Crystallographic Society of Japan*, **39,** 78–82.

Okamoto, K., Liou, J. G. & Ogasawara, Y., 2000. Petrology of the diamond-grade eclogite in the Kokchetav Massif, northern Kazakhstan. *Island Arc*, **9,** 379–399.

Pal'yanov, Y. N., Sokol, A. G., Borzdov, Y. M. & Khokhryakov, A. F., 2002. Fluid-bearing alkaline carbonate melts as the medium for the formation of diamonds in the Earth's mantle: an experimental study. *Lithos*, **60,** 145–159.

Pal'yanov, Y. N., Sokol, A. G., Borzdov, Y. M., Khokhryakov, A. F. & Sobolev, N. V., 1999. Diamond formation from mantle carbonate fluids. *Nature*, **400,** 417–418.

Parkinson, C. & Katayama, I., 1999. Metamorphic microdiamond and coesite from Sulawesi, Indonesia: Evidence of deep subduction at the SE Sundaland margin. *EOS Transactions of the American Geophysical Union*, **80,** F1181.

Shatsky, V. S., Pal'yanov, Y. N., Sokol, A. G., Tomilenk, A. A. & Sobolev, N. V., 2001. Diamond formation in UHP metamorphic rocks: natural and experimental evidence. '*Fluid/Slab/Mantle Interactions and Ultrahigh-P Minerals*'. Abstracts of UHPM Workshop 2001. Waseda University, 6–10.

Shatsky, V. S., Sobolev, N. V. & Vavilov, M. A., 1995. *Diamond-Bearing Metamorphic Rocks of the Kokchetav Massif (Northern Kazakhstan) in Ultrahigh-Pressure Metamorphism* (eds Coleman, R. G. & Wang, X.). Cambridge University Press, pp. 427–455.

Sobolev, N.V. & Shatsky, V.S., 1990. Diamond inclusions in garnets from metamorphic rocks: a new environment for diamond formation. *Nature*, **343,** 742–746.

Stöckhert, B., Duyster, J., Trepmann, C. & Massonne, H.-J., 2001. Microdiamond daughter crystals precipitated from supercritical COH + silicate fluids included in garnet, Erzgebirge, Germany. *Geology*, **29,** 391–394.

Xu, S., Okay, A. I., Ji, S., Sengor, A. M. C., Su, W., Liu, Y. & Jiang, L., 1992. Diamond from the Dabie Shan metamorphic rocks and its implication for tectonic setting. *Science*, **256,** 80–82.

Yoshioka, N., Muko, A. & Ogasawara, Y., 2001. Extremely high diamond concentration in dolomite marble. '*Fluid/Slab/Mantle Interactions and Ultrahigh-P Minerals*'. Abstracts of UHPM Workshop 2001. Waseda University, 51–55.

Received 26 February 2002; revision accepted 11 September 2002.